



Theoretical Study of the Transition Capacitance of a Solar Cell as a Function of Temperature: Choice of a Mathematical Model for the Gap Band and the Intrinsic Concentration of Carriers

Oumar Diallo SADIO¹, Al Moustapha SAMOURA¹, Waly FALL¹, Fabe Idrissa BARRO²

¹Research Student, Department of Physics, Science Faculty of Dakar, University Cheikh Anta Diop of Dakar (UCAD), Dakar, Senegal.

²Research Professor, Department of Physics, Science Faculty of Dakar, University Cheikh Anta Diop of Dakar (UCAD), Dakar, Senegal.
oumar.sadio@yahoo.fr

ABSTRACT

Photovoltaic solar cells can be electrically characterized under several regimes including the dynamic frequency regime. With this regime, electrical quantities such as parallel capacitance, parallel resistance, and dynamic resistance are determined. In theory, these quantities depend on other parameters of the cell. In this study, the transition capacitance was studied as a function of temperature under forward bias in the dark. This transition capacitance forms with the diffusion capacitance the parallel capacitance of the cell. The study was done taking into account the temperature dependence of the intrinsic carrier concentration, the gap band, and the effective carrier mass. A discussion was made on the different existing models concerning the gap band and the intrinsic carrier concentration. For all the models, the gap energy decreases with increasing temperature while the intrinsic carrier concentration increases with increasing temperature. It was found that the transition capacitance increases with increasing bias voltage for a given temperature. It also increases with increasing temperature for a given voltage.

Keywords: Transition capacitance, Silicon, Gap band, intrinsic carrier concentration and Temperature

INTRODUCTION

Photovoltaic solar cells are the most important components of a photovoltaic solar energy system. However, it is with these cells that light is transformed into electricity, since the discovery of the photoelectric effect and the manufacture of the first real photovoltaic solar cell within the Bell Company where an efficiency of 6% was quickly obtained. Since then, several photovoltaic solar cell technologies have emerged. Research continues to be carried out for a better understanding of these cells. This research is most often characterizations among which we can cite the electrical characterization which allows the determination of electrical quantities. However, the electrical characterization can be done in several regimes which are the static regime, the temporal regime, and the dynamic frequency regime. With the dynamic frequency regime, we can determine the series resistance, the parallel resistance, or the parallel capacitance. The determination of the electrical parameters in a dynamic frequency regime makes it possible to know the state of degradation of the solar cell. Parallel capacitance is the parallel association of transition capacitance, diffusion capacitance, and bulk capacitance. In theory, bulk capacitance tends to be neglected in front of transition capacitance and diffusion capacitance because it is of the order of 50pF/cm² for Silicon and very low compared to other values of the bulk capacitance of other solar cell technologies. In the literature, most of the works most often concern diffusion capacitance and transition capacitance. Jean-Paul Kleider et al reviewed the basic concepts of junction capacitance and the particularities related to very high-efficiency silicon heterojunction (SiHET) solar cells. By presenting both modeling and experimental results, they demonstrated that the conventional theory of transition capacitance based on the space charge depletion approximation, cannot reproduce the capacitance data obtained on SiHET cells. They found a discrepancy between the theoretical and experimental values obtained in the temperature and polarization dependence. They

demonstrated that this is not related to the amorphous nature of a-Si: H, but to the existence of a highly inverted c-Si surface layer which necessitates the consideration of minority carriers in the analysis of the junction capacitance [1]. R. Anil Kumar and M. S. Suresh, have designed a technique for measuring the capacitance of a solar cell in the time domain. The measurements were carried out on GaAs/Ge and silicon BSFR solar cells at different cell voltages and are presented and compared with the equivalent charge capacitance derived from the impedance spectroscopy technique [2]. Hiranmoy Mandal and J. Nagaraju have measured the capacitance of GaAs/Ge and silicon BSFR solar cells at different temperatures under dark conditions. They used the triangular wave method which is a technique applicable in the frequency domain. With their method, they applied, on the solar cells, an external bias using a DC voltage and a small AC triangular wave signal of desired amplitude with variable frequencies. They then measured the resulting AC current and calculated the cell capacitance. They found that the GaAs/Ge solar cell showed only a transition capacitance throughout its operating voltage while the silicon solar cell (BSFR) showed both transition and diffusion capacitances [3]. In theory, the transition capacitance occurs following the separation of charges in the space charge region at the junction of a photovoltaic solar cell. The phenomenon forming at the junction leads some authors to call it junction capacitance. However, the transition capacitance is related to the space charge region and behaves similarly to the electrical capacitance of a capacitor. It is often studied in dynamic frequency regimes, especially during voltage variation. This paper presents the theoretical study of the transition capacity taking into account the temperature dependence of intrinsic carrier concentration and the band gap of Silicon.

MODELING AND THEORETICAL ANALYSIS

Mathematical model of transition capacity

The transition capacity is given by:

$$C_T = \left| \frac{dQ}{dV_d} \right| = \frac{B}{(V_0 - V_d)^{1/2}} \quad (1)$$

Where B is a constant, V_0 is the junction voltage, and V_d the applied voltage.

The values of the junction voltage V_0 and the constant B can also be calculated from the doping levels in the n and p regions.

$$V_0 = \frac{kT}{q} \ln \left[\frac{N_A N_D}{n_i^2} \right] \quad (2)$$

$$B = A \sqrt{\frac{qN\varepsilon_0\varepsilon_r}{2}} \quad (3)$$

$$\frac{1}{N} = \frac{1}{N_A} + \frac{1}{N_D} \quad (4)$$

Where k is the Boltzmann constant, T is the temperature in K, q is the electron charge ($q = 1.6 \cdot 10^{-19}$ C), A is the surface area of the cell ($A = 9 \cdot 10^{-2} m^2$), ε_0 is the permittivity of vacuum ($\varepsilon_0 = 8,854 \cdot 10^{-12} F/M$), ε_r is the relative permittivity of the material ($\varepsilon_r = 11.9$ for Silicon), N_A is the doping concentration in the p-zone ($N_A = 1 \cdot 10^{21} \cdot m^{-3}$ for Silicon), N_D is the doping concentration in the n-zone ($N_D = 1 \cdot 10^{25} \cdot m^{-3}$ for Silicon), n_i is the intrinsic concentration of charge carriers in the solar cell base.

Mathematical model of the intrinsic concentration of charge carriers

The transition capacitance depends on the intrinsic density of charge carriers. The latter intrinsically depends on the cell temperature. In the literature, several values have been proposed. However, over time, the value of n_i changes, and authors such as Green, Sproul, Misiakos, and Altermatt have made changes to this value at 300K.

Green, is one of the authors who revised the value of n_i . Referring to a critical analysis of resistivity measurements, he brought it from $1,45 \cdot 10^{10} cm^{-3}$ to $1,08 \cdot 10^{10} cm^{-3}$ [4].

Later, Sproul and colleagues refined this value using specially designed cells to measure n_i and obtained a value of $1,00 \cdot 10^{10} cm^{-3}$ [5].

A new value, $9,70 \cdot 10^9 cm^{-3}$, was published shortly after by Misiakos, obtained from capacitance measurements on diodes biased under strong injection. However, in the literature authors reveal that the most frequently used value remains that proposed by Sproul [6].

Sproul's value has recently been corrected by Altermatt to $9,65 \cdot 10^9 cm^{-3}$, taking into account bandgap narrowing (BNG), which allowed Misiakos' and Sproul's values to be matched. The usually recommended value of 300 K is that obtained by Altermatt [7].

After this brief history on the real value of n_i at 300K, we will present a re-evaluation of n_i , which depends on the temperature, while taking into account the narrowing of the band gap. In doing so, a selection of the band gap model will be made since the latter also depends on the temperature. A critical analysis of the underlying theory will be carried out.

Mathematical aspect of the temperature dependence of n_i

The following equation gives the expression of the intrinsic density of charge carriers as a function of temperature.

$$n_i^2 = N_C(T)N_V(T)\exp\left[\frac{E_g^0(T)}{kT}\right] \quad (6)$$

Where: N_C and N_V are the effective densities of states in the conduction band and the valence band respectively, E_g^0 is the intrinsic band gap of Silicon and k is the Boltzmann constant.

The expressions of N_C and N_V are given by the following equations:

$$N_C = 2 \left(\frac{2\pi m_{dc}^* kT}{h^2} \right)^{\frac{3}{2}} \quad (7)$$

$$N_V = 2 \left(\frac{2\pi m_{dv}^* kT}{h^2} \right)^{\frac{3}{2}} \quad (8)$$

Where m_{dc}^* and m_{dv}^* are the effective masses of the densities of states in the conduction band and the valence band respectively and h is Planck's constant.

Using the physical constants recommended by Peter J. et al., equations (7) and (8) become:

$$N_C = 4.83 \times 10^{15} \left(\frac{m_{dc}^*}{m_0} \right)^{\frac{3}{2}} T^{\frac{3}{2}} \quad (9)$$

$$N_V = 4.83 \times 10^{15} \left(\frac{m_{dv}^*}{m_0} \right)^{\frac{3}{2}} T^{\frac{3}{2}} \quad (10)$$

Where m_0 is the electron mass.

m_{dc}^* and m_{dv}^* are obtained from the band diagram of Silicon in the first Brillouin zone.

$$m_{dc}^* = 6^{\frac{2}{3}} (m_t^* m_l^*)^{\frac{1}{3}} \quad (11)$$

$$m_{dv}^* = \left(m_{lh}^* \frac{3}{2} + m_{hh}^* \frac{3}{2} + \left(m_{so}^* \exp\left(\frac{-\Delta}{kT}\right) \right)^{\frac{3}{2}} \right)^{\frac{2}{3}} \quad (12)$$

Where m_t^* : is the transverse effective mass, m_l^* : is the longitudinal effective mass, m_{lh}^* : is the effective mass of the light hole band, m_{hh}^* : is the effective mass of the heavy hole band, m_{so}^* : is the effective mass of the split-off band, and Δ : is the energy between this band and the two previous ones.

It is possible to measure effective masses experimentally but at temperatures close to absolute zero. This requirement comes from the fact that the required cyclotron observations require very high charge carrier mobility [8].

The effective masses of the densities of states in the conduction band and in the valence band depend on the temperature. It is convenient to represent the temperature dependence of m_{dc}^* and m_{dv}^* in order to model N_C and N_V . This will allow us to have a new expression for n_i .

m_{dc}^* has weak temperature dependence, unlike m_{dv}^* , this allows us to assume that the theoretical temperature dependence of m_{dc}^* follows from that of m_l^* and m_t^* . Theoretically, m_l^* is independent of temperature and its value has been calculated with an accuracy of 4 K. Green proposed a model for the calculation of m_t^* given by equation (13).

$$m_t^* = 0,9163 \times m_0 \quad (13)$$

$$m_l^* = 0,1905 \times m_0 \left(\frac{E_g^0(0)}{E_g^0(T)} \right) \quad (14)$$

Equation (13) can be rewritten as equation (14)

A degree 3 extrapolation of the quotient of the second member of equation (11), made on the basis of the Passler model, allows us to have a simple expression of the ratio $\frac{m_l^*}{m_0}$.

$$\left(\frac{m_{dc}^*(T)}{m_0} \right)^{\frac{3}{2}} = A_C T^3 + B_C T^2 + C_C T + D_C \quad (16)$$

Where $A_C = -4,609.10^{-10}$, $B_C = -6,753.10^{-7}$, $C_C = -1,312.10^{-5}$ et $D_C = 1,094$

m_{dv}^* has a strong dependence on temperature. By making a polynomial approximation of degree 3 of equation (12) with Sproul data, we obtain a polynomial for m_{dv}^* .

$$\left(\frac{m_{dv}^*(T)}{m_0} \right)^{\frac{3}{2}} = A_V T^3 + B_V T^2 + C_V T + D_V \quad (17)$$

Where $A_V = 2,525.10^{-9}$, $B_V = -4,689.10^{-6}$, $C_V = -3,376.10^{-3}$ et $D_V = 3,426.10^{-1}$

In the literature, all models of the intrinsic charge carrier density have the form given by the following equation:

$$n_i = AT^B \exp\left(\frac{-C}{T}\right) \quad (18)$$

The coefficients A, B and C depend on the existing models.

The challenge behind the expression of n_i given by equation (17) is the choice of the model of the intrinsic band gap because, in the literature, there are many models of this band.

Band gap model

The authors Bludau *et al.* and Macfarlane *et al.* [9, 10], were the first to carry out experimental work on the band gap. Currently, the models presented in the literature, and dealing with the band gap are made on the basis of the works of Bludau and Macfarlane. However, three models are most often used. His models are the works of Thurmond, Alex, and Pässler [11, 12, 13, 14].

The models of Thurmond and Alex follow the following equation:

$$E_g^0(T) = E_g^0(0) - \frac{\alpha T^2}{T + \beta} \tag{19}$$

Where α is expressed in $eV \cdot K^{-1}$ and β in K.

The two assumptions of equation (III-16) are that the energy gap must be inversely proportional to T at high temperature and proportional to T² at low temperature. The use of this equation is justified by the fact that it adequately represents the experimental results of M. B. Panish *et al.*

The Pässler model follows the following equation:

$$E_g^0(T) = E_g^0(0) - \alpha \theta \left[\gamma + \frac{3\Delta^2}{2} \left(1 + \frac{\pi^2}{3(1+\Delta^2)} \chi^2 + \frac{3\Delta^2-1}{4} \chi^3 + \frac{8}{3} \chi^4 + \chi^6 - 1 \right)^{\frac{1}{6}} \right] \tag{20}$$

Where: α represents the limit at the slope level when T tends to infinity, θ is the average temperature of the phonons, Δ is the degree of dispersion of the phonons, specific to the material, γ depends on Δ , θ , and T. Its expression is given by the following equation:

$$\gamma = \frac{1-3\Delta^2}{\exp\left(\frac{\theta}{T}\right)-1} \tag{21}$$

RESULTS AND DISCUSSION

Justification of the model chosen for the band gap

Although the gap between the parameters of the three models is small, there is a difference between these three models (Figure 1).

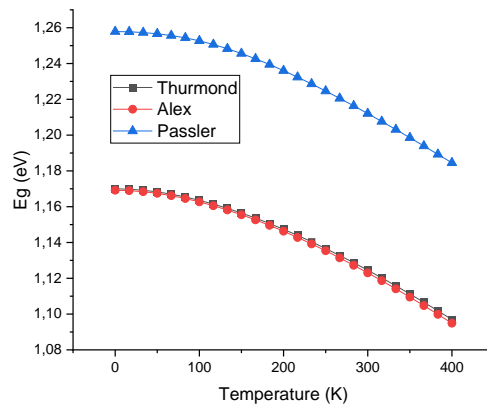


Figure 1: Band gap model as a function of temperature

However, to make a relevant analysis between these three models, one can consider the ratios between each model and the Pässler model as shown in Figure 2.

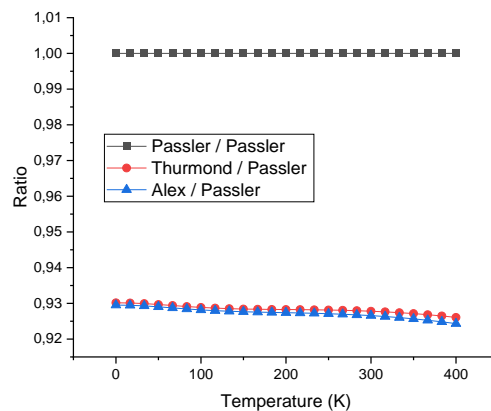


Figure 2: Band gap ratio of the models compared to the Pässler model

In the Figure 2, the deviation does not exceed unity and is of the order of 0.7 at low temperature and 0.8 at high temperature. These observations can be misleading because the intrinsic charge carrier density depends on the band gap but, it may well not follow the same trends given by the models of this band. Let us analyze more closely the implication of the band gap models on the model of the intrinsic charge carrier density. The unreality of the extremely wide dispersion regime implied by the Varshni model [15], and which has never been observed experimentally is the proof of the greater accuracy of the Pässler model. For low temperatures, we observe a tendency of $E_g(T)$ towards the asymptote $E_{g_lim}(0) - \alpha T$, where α is the slope of this asymptote and $E_{g_lim}(0)$ is the intersection of this asymptote with the y-axis at 0K. According to the Pässler model, the renormalization energy is defined as $E_{lim}(0) - E_g(T)$ and is equal to $\alpha\theta/2$ in the Varshni model. This means that the parameter α and the renormalization energy are overestimated in the Thurmond and Alex models. However, in the further study of the junction capacitance and in the choice of the intrinsic carrier density model, we will use the Alex model for the band gap. There is no motivation behind this choice.

We notice a decrease in the band gap as the temperature increases. This behavior is expected given the dependence of E_g on temperature with the Alex model. However, the band gap values for the Thurmond model and the Passler model have not been calculated. According to equation 19, the Thurmond and Alex models follow the same mathematical law in dependence on temperature. This suggests for the Thurmond model, a variation similar to that of the Alex model, the only difference will be in the values obtained.

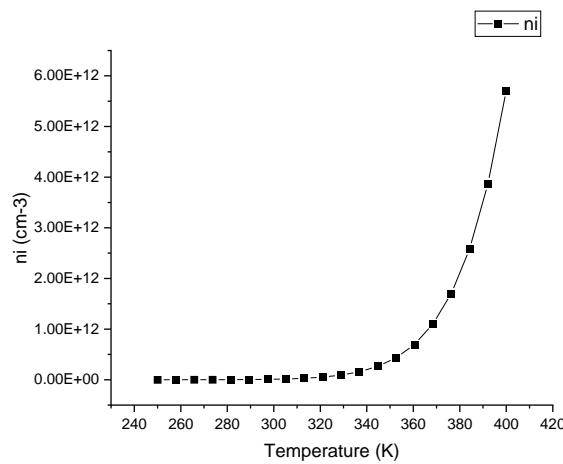


Figure 3: Variation of the intrinsic concentration of charge carriers as a function of temperature for the Sproul model

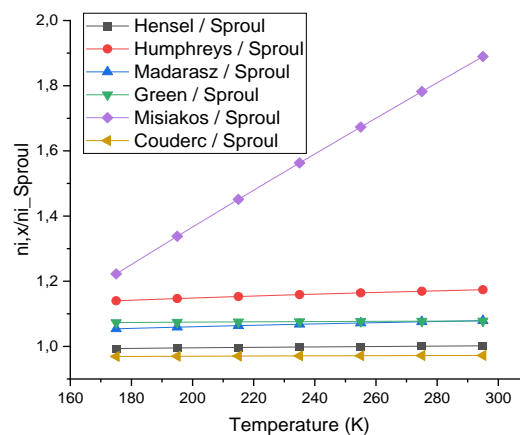


Figure 4: Ratio of different models with the Sproul model

Figure 3 shows that the intrinsic charge carrier density remains relatively low at low temperatures (250K to about 320K). From 320K onwards, it begins to increase rapidly and exponentially. This rapid increase in density with temperature is expected, because the thermal generation of electron-hole pairs increases with temperature.

However, at high temperatures, there is more thermal energy available to excite electrons from the valence band to the conduction band. The analyses made in Figure 3 suggest that the Sproul model uses specific band gap parameters and constants that produce physically reasonable results. Figure 4 plots the ratios of the intrinsic charge carrier concentrations of the other models to the Sproul model as a function of temperature. It allows us to make a comparison of the relative accuracy of the different models. His analysis reveals among other things: a consistency of the models at different temperatures, a divergent behavior of the Misiakos model [16] and ratios close to unity except that of Misiakos. Concerning the consistency of the models, the graphs of the Green, Couderc, Madarasz, Humpheys and Hensel models [4,17, 18, 19, 20] are relatively constant and close to unity. Based on this observation, we can say that the predictions of the intrinsic density of charge carriers for these models are quite similar to that of the Sproul model over the entire temperature range. This reveals a consistency between these models which do not deviate much from that of Sproul. Concerning the divergent behavior of the Misiakos model, its curve increases significantly with temperature, exceeding 1.6 at 300K. This indicates that the Misiakos model predicts a much higher intrinsic concentration than the Sproul model at higher temperatures, suggesting that the Misiakos model is more sensitive to temperature. This increased sensitivity to temperature compared to other models may be due to the model parameters. The mathematical model of the intrinsic charge carrier density sheds light on the temperature dependence of the transition capacitance. This will allow further analysis of the variation of the transition capacitance with respect to temperature. Figure 5 shows the variation of the transition capacitance as a function of the applied voltage for a temperature of 300K.

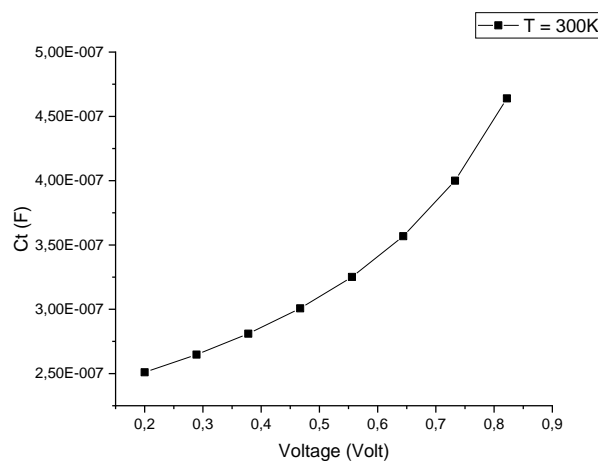


Figure 5: Variation of the transition capacitance C_t as a function of the applied voltage

In Figure 6, it is clear that the curve increases rapidly as the voltage increases. This simply indicates a significant change in the transition capacitance at higher voltages. The bias voltage creates a potential difference that is applied to the depletion region. This voltage brings a change to the height of the potential barrier that gradually decreases as this bias voltage increases. For a dynamic analysis and with respect to the photovoltaic solar cell, the transition capacitance plays a role in the cell's response to a voltage change. For a forward-biased solar cell, the generated charge carriers are separated by the junction, which reacts according to the voltage. Thus, the transition capacitance influences the speed at which the junction can react to voltage changes [21]. Although this effect is noticeable in high-frequency devices, its impact is less significant in a solar cell, where the priority is the efficient collection of charges generated by light. Basically, the relationship between junction capacitance and bias voltage can be explained by several factors. First, there is the doping of the semiconductor in terms of dopant concentration and dopant type: the dopant concentration influences the width of the space charge region. However, for an applied voltage, high doping can reduce the width of this region. Second, there is the nature of the semiconductor material in terms of its band gap: for an applied bias voltage, a material with a wider band gap will have a different space charge region width. Finally, there is the presence of defects and impurities in the fabrication of the semiconductor material: defects tend to trap charge carriers, thus changing their distributions in this region. Impurities, on the other hand, tend to introduce additional energy levels into the band gap. This affects the recombination and generation of charge carriers. The study of the influence of temperature on semiconductors allows us to better understand the behavior of charge carriers when the temperature changes. This also allows us to better understand their properties. Since the junction capacitance is linked to the storage of carriers in the space charge region, it is obvious that temperature has an influence on this capacitance. Although the junction capacitance predominates at low voltage, in this section, we present the results of the calculations as a function of temperature over a wide excitation voltage range (0.2 Volts-0.8 Volts) (Figure 6).

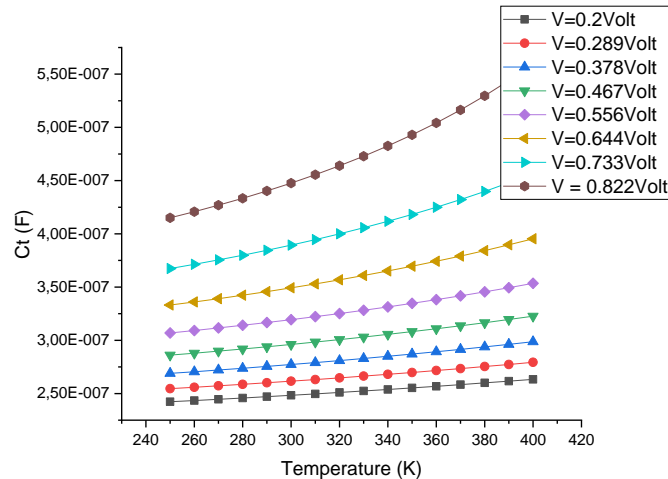


Figure 6: Variation of transition capacitance as a function of temperature for different bias voltages

In Figure 6, it is observed that for an applied voltage, the values of the transition capacitance increase with increasing temperature. This variation is related to the concentration of charge carriers at two levels. First, the concentration of free charge carriers in the cell is affected by temperature. However, at low temperatures, there is not enough thermal energy to excite a large number of electrons from the valence band to the conduction band. This results in a decrease in the concentration of charge carriers, thus leading to a decrease in the width of the space charge region. It should be noted that a low temperature of the solar cell, which is made of doped semiconductors, promotes a reduction in collision and recombination [21]. Second, the variation can also be due to the influence of the band gap width on the intrinsic concentration of charge carriers. However, the energy of the latter is reduced as the temperature increases [4]. This leads to an exponential increase in the intrinsic n_i concentration which at the same time increases the concentration of minority charge carriers. This increase in the concentration of minority charge carriers leads to an imbalance in the semiconductor. To restore the balance, the width of the space charge region narrows. This narrowing of the width of the space charge region thus leads to an increase in the transition capacity. It is clear that for a voltage applied to the photovoltaic solar cell, the decrease in temperature has consequences on the transition capacity. The latter quantifies the charges stored in the depletion zone. These consequences involve the storage of charges. This is caused by the concentration and reduced mobility of the charge carriers, thus limiting the amount of charges that can be stored in the junction.

CONCLUSION

The electrical parameters of solar cells in dynamic frequency regime are the subject of much research in practice and theory. This paper is a theoretical study of the junction capacitance with emphasis on mathematical models of parameters such as intrinsic carrier concentration and gap. Under the influence of temperature and forward bias voltage, the intrinsic carrier concentration is found to be temperature dependent as well as the gap. The transition capacitance is dependent on both the transition voltage and temperature. It increases with increasing voltage on the one hand and with increasing temperature on the other hand. Its increase with increasing bias voltage is due to the doping of the semiconductor with respect to dopant concentration and dopant type, the nature of the semiconductor material with respect to its band gap, and the presence of defects and impurities in the fabrication of the semiconductor material. Compared to temperature, its increase is due to the concentration of free charge carriers in the cell and the influence of the band gap width on the intrinsic concentration of charge carriers.

REFERENCES

- [1]. JP Kleider, J Alvarez and A Brézard-Oudot, Revisiting the theory and usage of junction capacitance: Application to high efficiency amorphous/crystalline silicon heterojunction solar cells, *Solar Energy Materials & Solar Cells*, 2015, 135, 8-16.
- [2]. R Anil Kumar, M S Suresh and J Nagarajua, Time domain technique to measure solar cell capacitance, *Review of Scientific Instrument*, 2003, 74 (7), 3516-3519.
- [3]. H Mandal and J Nagaraju, GaAs/Ge and silicon solar cell capacitance measurement using triangular wave method, *Solar Energy Materials & Solar Cells*, 2007, 91, 696-700
- [4]. M A Green, Intrinsic concentration, effective densities of states, and effective mass in silicon, *Journal of Applied Physics*, 1990, 67 (6), 2944-2954.

-
- [5]. A B Sproul and M A Green, Intrinsic carrier concentration and minority carrier mobility of silicon from 77 to 300 K, *Journal of Applied Physics*, 1993, 73 (3), 1214-1225.
 - [6]. K Misiakos and D Tsamakis, Accurate measurements of the silicon intrinsic carrier density from 78 to 340 K, *Journal of Applied Physics*, 1993, 74 (5), 3293-3297.
 - [7]. P P Altermatt, A Schenk, F Geelhaar, and G Heiser, "Reassessment of the intrinsic carrier density in crystalline silicon in view of band-gap narrowing," *Journal of Applied Physics*, 2003, 93 (3), 1598-1604.
 - [8]. M Godlewski, W M Chen and B Monemar, Optical detection of cyclotron resonance for characterization of recombination processes in semiconductors, *Critical Reviews in Solid State and Material Sciences*, 1994, 19 (4), 241-301.
 - [9]. W Bludau, A Onton, and W Heinke, Temperature dependence of the band gap of silicon, *Journal of Applied Physics*, 1974, 45 (4), p. 1846-1848.
 - [10]. G Macfarlane, T McLean, J Quarrington, and V Roberts, Fine Structure in the absorption-edge spectrum of Si, *Physical Review*, 1958, 111 (5), 1245-1254.
 - [11]. C Thurmond, The standard thermodynamic functions for the formation of electrons and holes in Ge, Si, GaAs, and GaP, *Journal of the Electrochemical Society*, 1975, 122 (8), 1133-1141.
 - [12]. V Alex, S Finkbeiner, and J Weber, Temperature dependence of the indirect energy gap in crystalline silicon, *Journal of Applied Physics*, 1996, 79 (9), 6943-6946.
 - [13]. R Pässler, Dispersion-related description of temperature dependencies of band gaps in semiconductors, *Physical Review B*, 2002, 66, 85201.1-85201.18.
 - [14]. R Pässler, Semi-empirical descriptions of temperature dependences of band gaps in semiconductors, *Physica Status Solidi (B)*, 2003, 236 (3), 710-728.
 - [15]. Y Varshni, Temperature dependence of the energy gap in semiconductors, *Physica*, 1967, 34 (1), 149-154.
 - [16]. K Misiakos and D Tsamakis, Accurate measurements of the silicon intrinsic carrier density from 78 to 340 K, *Journal of Applied Physics*, 1993, 74 (5), 3293-3297.
 - [17]. R Couderc, M Amara and M Lemiti, Reassessment of the intrinsic carrier density temperature dependence in crystalline silicon, *J. Appl. Phys.*, 2014, 115 (14), 149901-149901-1
 - [18]. F L Madarasz, J E Lang, and P M Hemeger, Effective masses for nonparabolic bands in p-type silicon, *Journal of Applied Physics*, 1981, 52 (7), 4646-4648.
 - [19]. R G Humphreys, Valence band averages in silicon : Anisotropy and nonparabolicity, *Journal of Physics C : Solid State Physics*, 1981, 14, 2935-2942.
 - [20]. J Hensel and G Feher, Cyclotron Resonance Experiments in Uniaxially Stressed Silicon : Valence Band Inverse Mass Parameters and Deformation Potentials, *Physical Review*, 1963, 129 (3), 1041-1062.
 - [21]. F Recart and A Cuevas, Application of Junction Capacitance Measurements to the Characterization of Solar Cells, *IEEE Transactions on Electron Devices*, 2006, 53 (3), 442-448.